

Communication

Recess-Free E-Mode AlGaIn/GaN MIS-HFET with Crystalline PEALD AlN Passivation Process

Won-Ho Jang , Jun-Hyeok Yim, Hyungtak Kim  and Ho-Young Cha * 

School of Electronic and Electrical Engineering, Hongik University, 94 Wausan-ro, Mapo-gu, Seoul 04066, Republic of Korea; jwh8904@mail.hongik.ac.kr (W.-H.J.); jhgjhg4@g.hongik.ac.kr (J.-H.Y.); hkim@hongik.ac.kr (H.K.)

* Correspondence: hcha@hongik.ac.kr

Abstract: We utilized a plasma-enhanced atomic layer deposition (PEALD) process to deposit an AlN passivation layer on AlGaIn/GaN surface to enhance the polarization effects, which enabled the fabrication of an enhancement-mode (E-mode) AlGaIn/GaN metal-insulator-semiconductor heterojunction field-effect transistor (MIS-HFET) without the need for a gate recess process. The AlN film deposited by PEALD exhibited a crystalline structure, not an amorphous one. The enhanced polarization effect of introducing the PEALD AlN film on a thin AlGaIn barrier was confirmed through electrical analysis. To fabricate the E-mode AlGaIn/GaN MIS-HFET, the PEALD AlN film was deposited on a 4.5 nm AlGaIn barrier layer and then a damage-free wet etching process was used to open the gate region. The MIS-gate structure was formed by depositing a 15 nm plasma-enhanced chemical vapor deposition (PECVD) silicon dioxide (SiO₂) film. The fabricated thin-AlGaIn/GaN MIS-HFET demonstrated successful E-mode operation, with a threshold voltage of 0.45 V, an on/off ratio of approximately 10⁹, a specific on-resistance of 7.1 mΩ·cm², and an off-state breakdown voltage exceeding 1100 V.

Keywords: AlN; AlGaIn/GaN heterojunction; thin-AlGaIn; enhancement-mode; plasma-enhanced atomic layer deposition



Citation: Jang, W.-H.; Yim, J.-H.; Kim, H.; Cha, H.-Y. Recess-Free E-Mode AlGaIn/GaN MIS-HFET with Crystalline PEALD AlN Passivation Process. *Electronics* **2023**, *12*, 1667. <https://doi.org/10.3390/electronics12071667>

Academic Editors: Weijun Luo and Yangfeng Li

Received: 21 February 2023

Revised: 22 March 2023

Accepted: 30 March 2023

Published: 31 March 2023



Copyright: © 2023 by the authors. Licensee MDPI, Basel, Switzerland. This article is an open access article distributed under the terms and conditions of the Creative Commons Attribution (CC BY) license (<https://creativecommons.org/licenses/by/4.0/>).

1. Introduction

Gallium nitride (GaN) is a material with a wide energy bandgap (~3.45 eV), which offers both a high critical electric field and high electron mobility, enabling high breakdown voltage and fast switching speed [1,2]. This makes it a highly attractive semiconductor material for use in various applications, including power electronics and radio frequency (RF) devices. Compared to conventional Si-based semiconductors, GaN-based semiconductors have the potential to overcome the material limitations that have previously hampered electronic device performance. One specific area of research in which GaN-based semiconductors have shown significant promise is in high-efficiency power conversion applications that require high breakdown voltage and fast switching speed.

In AlGaIn/GaN heterojunction structures, the difference in crystal structure and lattice constant causes strong polarization effects that enable the formation of a high-density two-dimensional electron gas (2DEG) channel between AlGaIn and GaN layers without the need for a doping process [3]. However, the presence of the high-density 2DEG channel makes it challenging to achieve enhancement-mode (E-mode) operation, which is highly desired for power devices given the simplicity of gate driver circuits and safe operating conditions.

To address this issue, researchers have investigated P-GaN gated AlGaIn/GaN heterojunction field-effect transistors (HEFTs) and recessed metal-insulator-semiconductor (MIS)-HFETs for achieving E-mode operation [4–6]. However, the critical fabrication process steps for both devices, such as plasma etching and passivation processes, can induce

surface damage and create trap states that degrade the dynamic characteristics during the switching operation. In addition, the controllability of the etching process is also critical.

To resolve these issues, researchers have proposed the use of a thin-AlGa_N/Ga_N heterostructure [7–11]. When the AlGa_N barrier layer is thin enough to deplete the 2DEG channel, the E-mode device can be achieved without the need for an etching process. However, the drawback of the thin-AlGa_N barrier layer is the limited channel formation outside the gate region, which must be compensated for by a proper passivation film. Several studies have reported that the proper passivation process can increase the 2DEG carrier density in thin-AlGa_N barrier structures [8–10].

In this study, we developed a plasma-enhanced atomic layer deposition (PEALD) AlN passivation process that resulted in the formation of a crystalline AlN film on top of the AlGa_N surface, rather than an amorphous film. The crystalline AlN film on the thin AlGa_N barrier layer enhanced the polarization effects, increasing the 2DEG channel density. Another potential method that could be considered for enhancing the crystallinity of the AlN film is in-situ AlN epitaxial growth. However, this approach presents challenges in terms of selective removal of the AlN layer without attacking the underlying thin AlGa_N layer, as well as limited thermal budget during device fabrication. Therefore, an ex-situ AlN deposition process with a lower temperature is preferred from a device fabrication perspective. The PEALD AlN process provides more flexibility during the device fabrication in comparison with the in-situ epitaxial growth. The PECVD AlN process developed in this study was successfully employed to fabricate an E-mode AlGa_N/Ga_N MIS-HFET without a plasma etching process, making it a promising solution for the challenges faced in device manufacturing.

2. Experiments Results

The process of depositing an AlN film was carried out using Trimethylaluminum (TMA) and NH₃ gas as precursors in a PEALD system. The optimum AlN deposition conditions were TMA feeding time of 0.1 s, NH₃ plasma time of 10 s, a pressure of 200 mTorr, and a chamber temperature of 330 °C, which resulted in a deposition rate of 1.1 Å per cycle, and a refractive index of 2.0. A detailed optimization report of various process conditions has been previously published [12].

To evaluate the quality of the AlN film, we deposited a 100 nm-thick AlN film onto an n-type Ga_N epitaxial layer grown on a SiC substrate and performed X-ray diffraction (XRD) measurements. The XRD pattern in Figure 1a revealed two distinct diffraction peaks at 2θ values of approximately 33° and 36°, which were assigned to the AlN (100) and AlN (002) peaks, respectively. These peaks correspond to the crystal planes of the hexagonal wurtzite structure of AlN. As shown in Figure 1b, the full width at half-maximum (FWHM) of the AlN (002) peak was measured to be 356 arcsec, which indicates the high crystalline quality of the deposited AlN film. The narrow FWHM of the AlN (002) peak is indicative of the high degree of structural perfection and crystallinity of the AlN film. X-ray photoelectron spectroscopy (XPS) measurements were conducted to analyze the film composition. The Al 2p, N 1s, and O 1s spectra were analyzed, as shown in Figure 2. The resulting atomic concentration of Al, N, and O were 46.8%, 41.1%, and 12.1%, respectively.

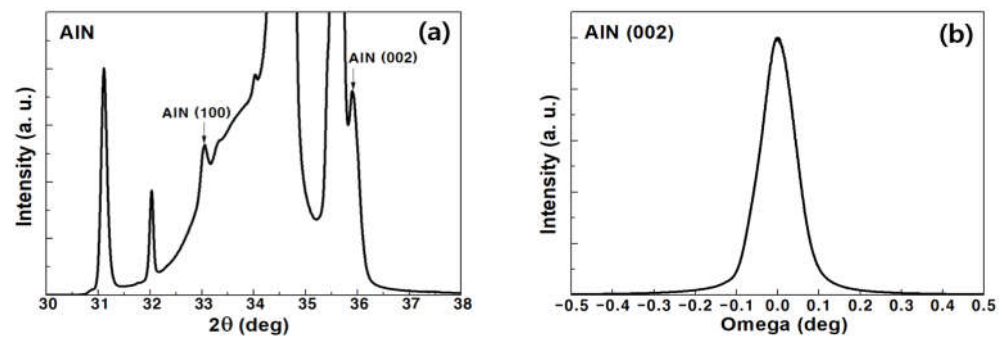


Figure 1. (a) XRD result and (b) rocking curve of AlN (002) plane of a 100 nm thick PEALD AlN film deposited on GaN surface.

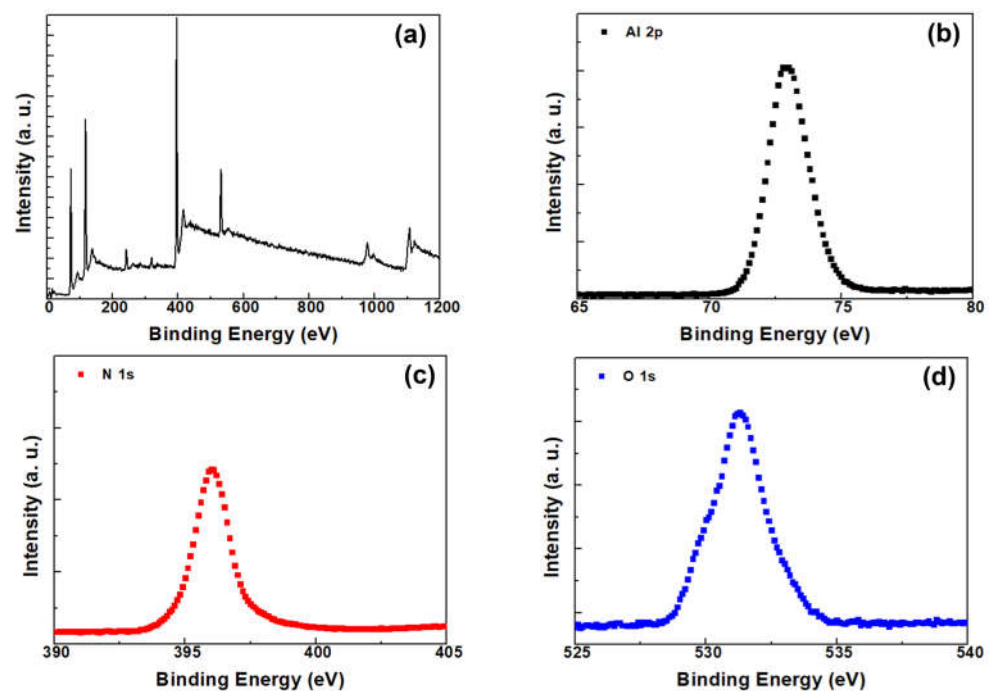


Figure 2. XPS spectra of PEALD AlN film; (a) wide-scan, (b) Al 2p, (c) N 1s, and (d) O 1s of the PEALD AlN film.

The AlN film was deposited using the same optimized deposition process on a thin-AlGaN/GaN heterostructure in which the AlGaN barrier layer was 4.5 nm thick. A high-resolution transmission electron microscopy (HRTEM) image was obtained from a cross-sectional view of the PEALD AlN film on the heterostructure, and is presented in Figure 3. The HRTEM image clearly indicates that the PEALD AlN film possesses a crystalline structure similar to that of the epitaxial layer, which is indicative of high film quality. This observation implies that the exceptional quality of the deposited AlN film not only significantly enhances the interface conditions between the AlN passivation film and the AlGaN barrier surface, but also enhances the polarization effects, thereby leading to an increase in the 2DEG carrier density.

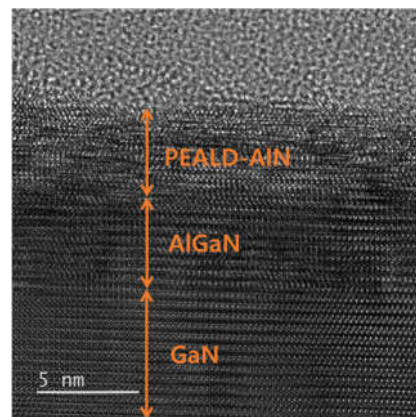


Figure 3. Cross-sectional HRTEM image of PEALD AlN film deposited on AlGaN/GaN heterostructure.

In Figure 4, the results of the TEM energy-dispersive X-ray spectroscopy (TEM-EDX) mapping of the PEALD-deposited AlN film on the AlGaN/GaN structure are displayed.

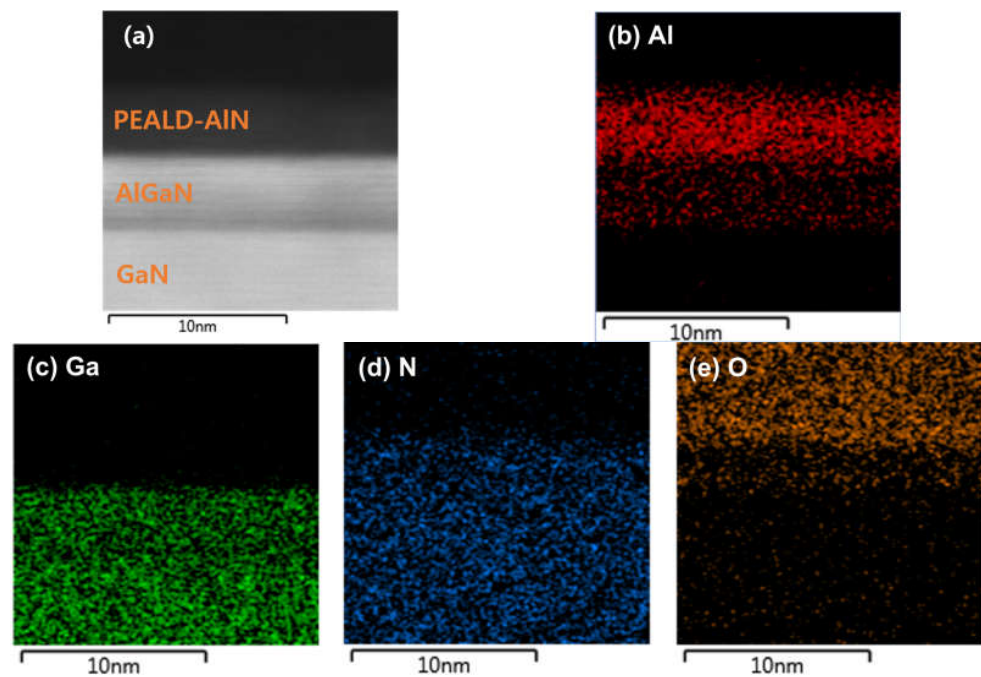


Figure 4. Element distribution of PEALD AlN film/AlGaN/GaN heterostructure analyzed by TEM-EDX mapping; (a) cross-sectional view, (b) aluminum, (c) gallium, (d) nitrogen, and (e) oxygen.

By providing detailed elemental information, the TEM-EDX mapping offers valuable insights into the precise distribution of each element in the layered structure. The mapping enables the clear identification of the boundaries between the PEALD AlN, AlGaN, and GaN layers based on their constituent elements.

To investigate the distribution of carriers along the depth and the interface quality, capacitance-voltage (C-V) measurements were conducted at 1 MHz for the sample with a 10 nm thick PEALD AlN film. The thickness of the barrier that includes the PEALD AlN film and the AlGaN barrier layer was confirmed by deriving the carrier distribution along the depth from the C-V characteristics, as shown in Figure 5a. The interface trap density was extracted using the Terman method [13]. As shown in Figure 5b, the interface trap density was in the order of $\sim 10^{12} \text{ cm}^{-2} \text{ eV}^{-1}$.

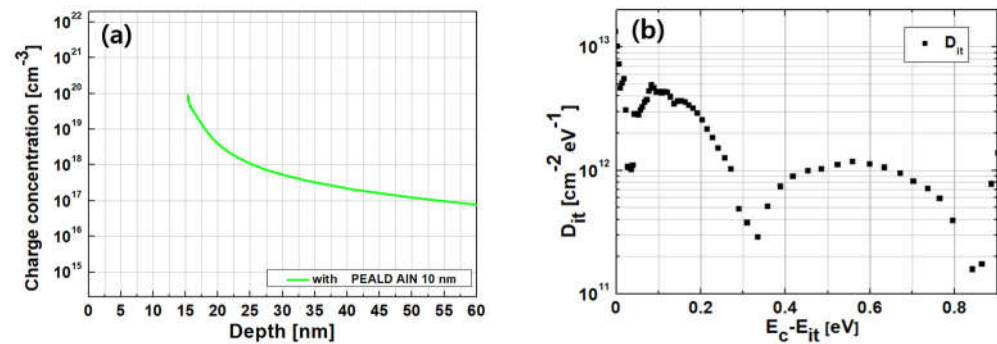


Figure 5. (a) Carrier distribution versus depth and (b) interface trap density extracted by Terman method.

The PEALD AlN deposition process was utilized in the fabrication of an E-mode AlGa_{0.2}N/GaN MIS-HFET. The epitaxial structure consisted of a 4.5 nm Al_{0.2}Ga_{0.8}N barrier layer, a 420 nm i-GaN channel layer, and a GaN buffer layer grown on a Si(111) substrate. To prepare the substrate for device fabrication, solvent and acid cleaning were carried out. Next, an ohmic metal stack composed of Ti/Al/Ni/Au was deposited and then annealed by rapid thermal annealing in N₂ ambient at 820 °C for 30 s. Mesa isolation was performed using a BCl₃/Cl₂-based plasma etching process, resulting in an etch depth of approximately 300 nm. Subsequently, a crystalline PEALD AlN film with a thickness of either 5 nm or 10 nm was deposited at 330 °C, followed by post-deposition annealing in an N₂ ambient at 500 °C for 5 min to enhance the film and interface qualities. A damage-free wet-etching process with a TMAH-based AZ300 solution was utilized to etch the PEALD AlN film in the gate foot region. For comparison, a reference sample was also fabricated without the PEALD AlN film. To complete the device structure, a 15 nm-thick PECVD SiO₂ layer was deposited as the gate dielectric and additional passivation. The SiO₂ film on the ohmic metal region was then etched using reactive ion etching with SF₆ gas, and a Mo/Au metal stack was evaporated for the gate and pad electrodes. Finally, post-metallization annealing was carried out at 400 °C in an O₂ ambient. The resulting device had a source-to-gate distance of 2 μm, a gate length of 4 μm, and a gate-to-drain distance of 11 μm, with a gate overhang length of 1 μm. Figure 6a,b illustrate the cross-sectional schematics of the fabricated thin-AlGa_{0.2}N/GaN MIS-HFET without and with the AlN film, respectively.

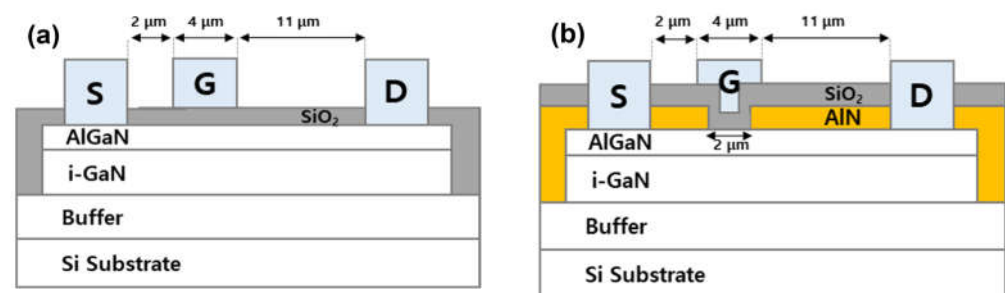


Figure 6. Cross-sectional schematics of thin-AlGa_{0.2}N/GaN MIS-HFETs fabricated (a) without and (b) with PEALD AlN film.

First, the current-voltage (I-V) characteristics between two ohmic contacts with different distances were measured in which no gate structure was formed between ohmic contacts. Figure 7a–c show the I-V characteristics obtained in a reference sample without the PEALD AlN film, a sample with a 5 nm PEALD AlN film, and a sample with a 10 nm PEALD AlN film, respectively. The reference sample exhibited no channel current, whereas samples with the AlN film exhibited significantly increased current flow. Because of the thin-AlGa_{0.2}N barrier layer, the 2DEG channel was not able to be formed enough. In comparison with the sample with a 5 nm PEALD AlN film, that with a 10 nm PEALD AlN film exhibited significantly higher current densities; the current density increased with

an increase in the AlN film thickness, which confirmed the enhanced polarization effects. At a bias of 5 V, the current density for a distance of 2 μm between ohmic contacts was 5×10^{-9} A/mm without the AlN film, and 0.18 mA/mm and 0.28 A/mm with 5 nm and 10 nm AlN films, respectively.

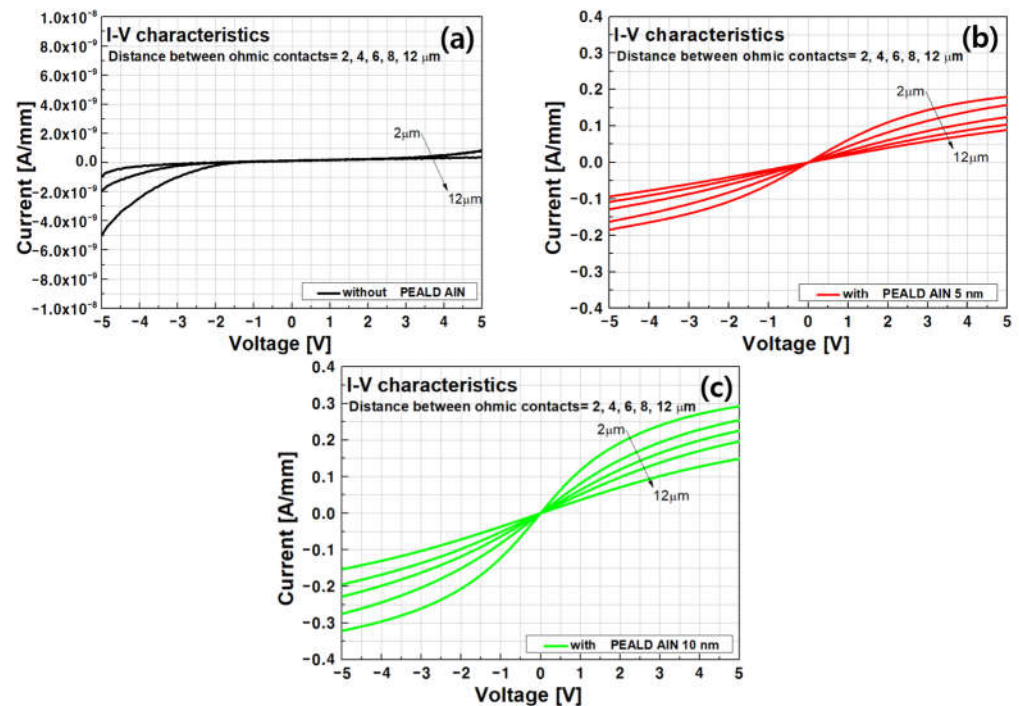


Figure 7. Current-voltage characteristics measured between two ohmic contacts with different distances; (a) reference sample without PEALD AlN film, (b) sample with a 5 nm thick PEALD AlN film, and (c) sample with a 10 nm thick PEALD AlN film.

Hall measurements were performed to investigate the electrical properties of the thin-AlGaIn/GaN heterostructure with different AlN thicknesses. The sheet resistance values for 5 nm and 10 nm AlN films were 1332 and 1012 Ω/sq , respectively, while the 2DEG densities for 5 nm and 10 nm AlN films were $4.1 \times 10^{12}/\text{cm}^2$ and $5.3 \times 10^{12}/\text{cm}^2$, respectively. The higher 2DEG density obtained with a thicker AlN film is attributed to the enhanced polarization effects. However, it is important to note that the thickness of the AlN layer on the AlGaIn/GaN surface should not exceed the critical thickness to avoid crack generation, which is not much thicker than 10 nm. The mobility values obtained with 5 nm and 10 nm PEALD AlN films were 1130 $\text{cm}^2/\text{V}\cdot\text{s}$ and 1160 $\text{cm}^2/\text{V}\cdot\text{s}$, respectively. The typical 2DEG mobility values for 20–25 nm AlGaIn barrier structures are approximately 1600 $\text{cm}^2/\text{V}\cdot\text{s}$ [14]. It is widely known that the mobility decreases as the AlGaIn barrier thickness decreases. Although the interface between PEALD AlN film and AlGaIn barrier layer may not be as perfect as an epitaxially grown structure, the mobility values obtained with PEALD AlN films in this study are compatible with AlGaIn/GaN structures with similar barrier thicknesses. Therefore, the results suggest that the PEALD AlN film can serve as an effective passivation layer for AlGaIn/GaN MIS-HFETs, thereby improving their overall performance.

Figure 8 shows the transfer I-V characteristics of the thin-AlGaIn/GaN MIS-HFET with varying PEALD AlN thicknesses. Figure 8a,b demonstrate that the thin-AlGaIn/GaN MIS-HFET fabricated without an AlN film failed to exhibit modulation characteristics. Conversely, the devices fabricated with the PEALD AlN film exhibited excellent transfer characteristics, with a low gate leakage current. The thin-AlGaIn/GaN MIS-HFET with a 5 nm-thick AlN film had a threshold voltage of 0.45 V (at 1 mA/mm), a maximum drain current density ($I_{D,\text{max}}$) of 85 mA/mm, and an on/off ratio of approximately 10^9 ,

as shown in Figure 8c,d. The device with a 10 nm-thick AlN film had the same threshold voltage of 0.45 V (at 1 mA/mm) with a higher maximum drain current density ($I_{D,max}$) of 170 mA/mm and an on/off ratio of approximately 10^9 , as shown in Figure 8e,f.

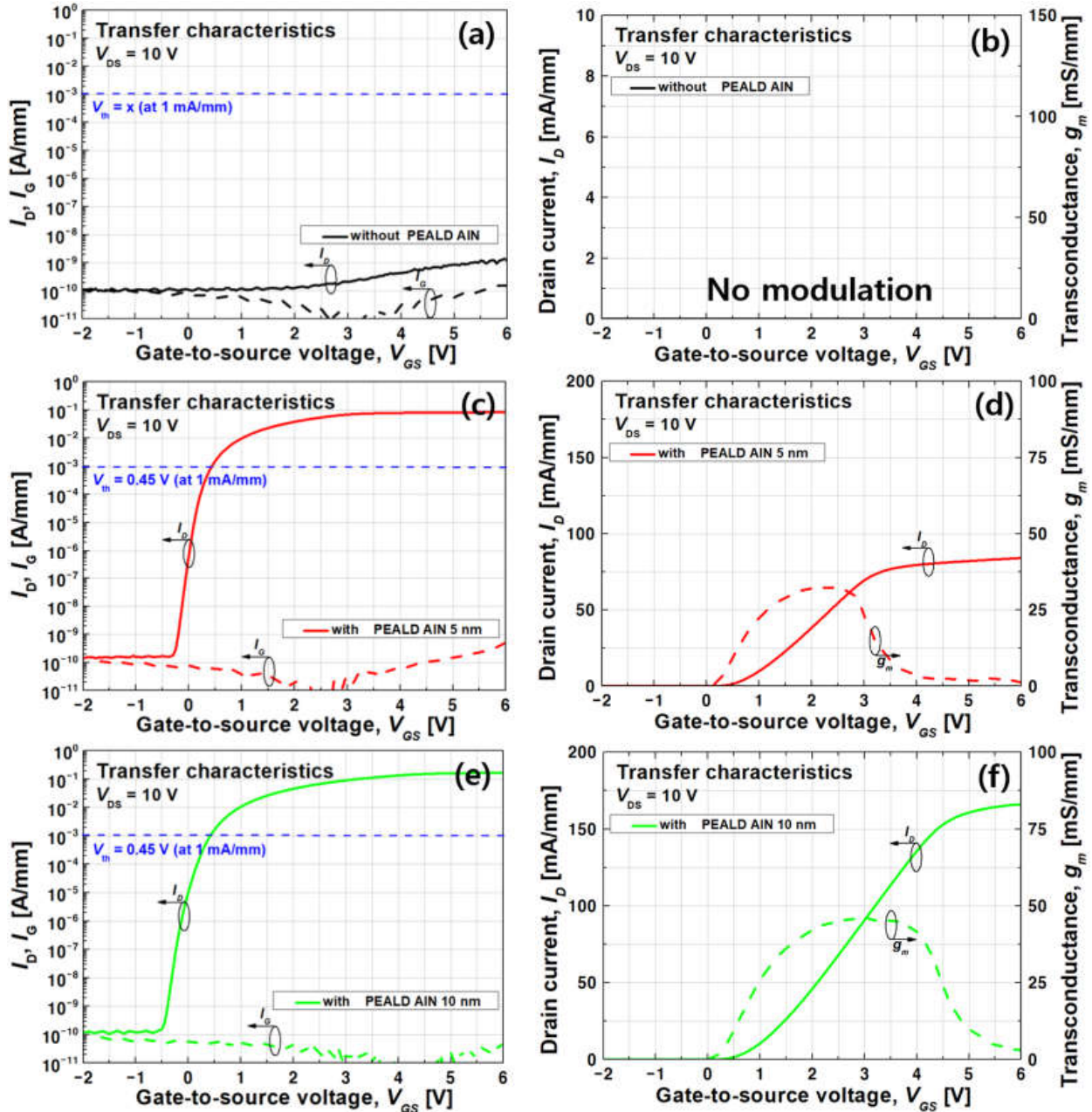


Figure 8. Transfer characteristics of fabricated thin-AlGaN/GaN MIS-HFETs; (a,b) reference device without PEALD AlN film, (c,d) device with a 5 nm thick PEALD AlN film, and (e,f) device with a 10 nm thick PEALD AlN film.

Due to the absence of a gate recess in the device fabrication process, it was anticipated that uniform threshold voltage characteristics would be obtained. To investigate the uniformity of threshold voltage characteristics, multiple devices located in different areas (four at the corners and one at the center) were measured in samples that consisted of 5 nm and 10 nm thick PEALD AlN films. The findings, as shown in Figure 9a,b, indicated that there was minimal variation among the different devices. It is suggested that the slight differences that were observed could be attributed to the SiO₂ MIS interface or other

processing issues. It is evident that both samples exhibited identical threshold voltage characteristics due to the identical configuration under the gate region.

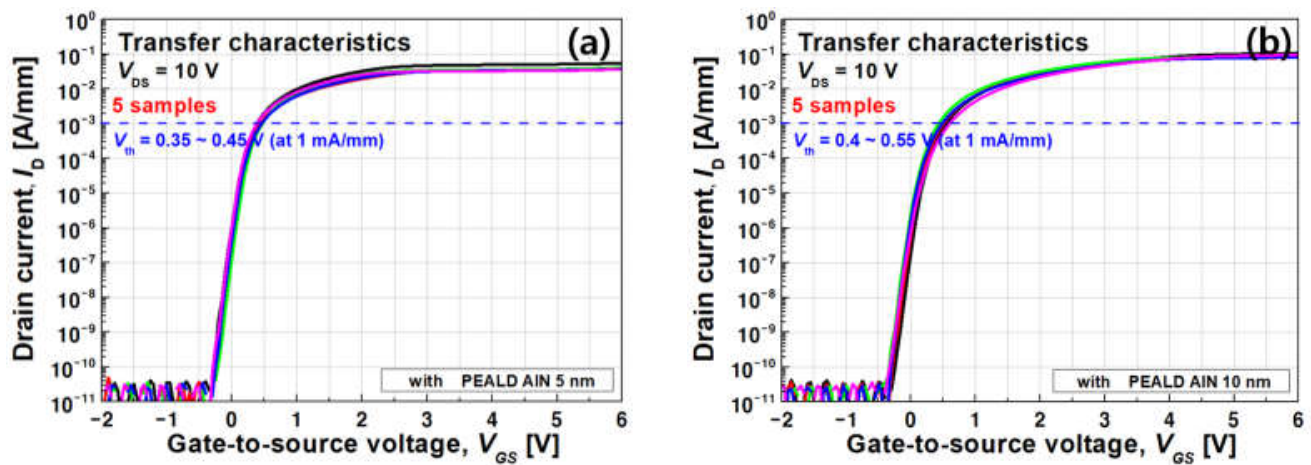


Figure 9. Threshold voltage characteristics obtained from multiple devices in samples with (a) 5 nm and (b) 10 nm AlN layers.

To investigate the hysteresis characteristics, C-V measurements were performed at 1 MHz on both PECVD SiO₂/AlGaIn/GaN and PEALD AlN/AlGaIn/GaN structures. The former is the MIS gate configuration that plays an important role in hysteresis in threshold voltage characteristics. As shown in Figure 10, the hysteresis values were 150 mV and 10 mV for the PECVD SiO₂/AlGaIn/GaN and PEALD AlN/AlGaIn/GaN structures, respectively. Both structures exhibited minimal hysteresis, indicating excellent interface conditions. Although still relatively small, slightly larger hysteresis was observed for the PECVD SiO₂/AlGaIn/GaN structure, which requires further optimization.

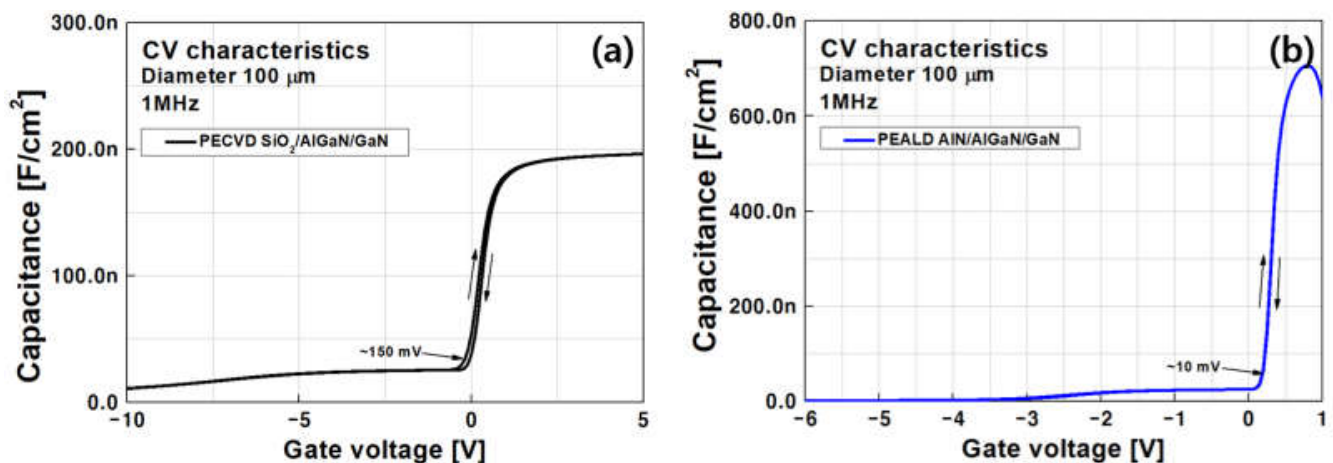


Figure 10. C-V hysteresis characteristics measured at 1 MHz for (a) PECVD SiO₂/AlGaIn/GaN and (b) PEALD AlN/AlGaIn/GaN structures.

The output current-voltage characteristics of the thin-AlGaIn/GaN MIS-HFETs are demonstrated in Figure 11. As expected, the device without an AlN film exhibited no current flow, whereas the devices with 5 nm and 10 nm AlN films showed good output characteristics. The devices with 5 nm and 10 nm AlN films achieved specific on-resistances of 20 and 7.1 mΩ·cm², respectively. The lower specific on-resistance observed in the device with a 10 nm AlN film is attributed to the higher 2DEG density outside the gate region, which is due to the enhanced polarization effects.

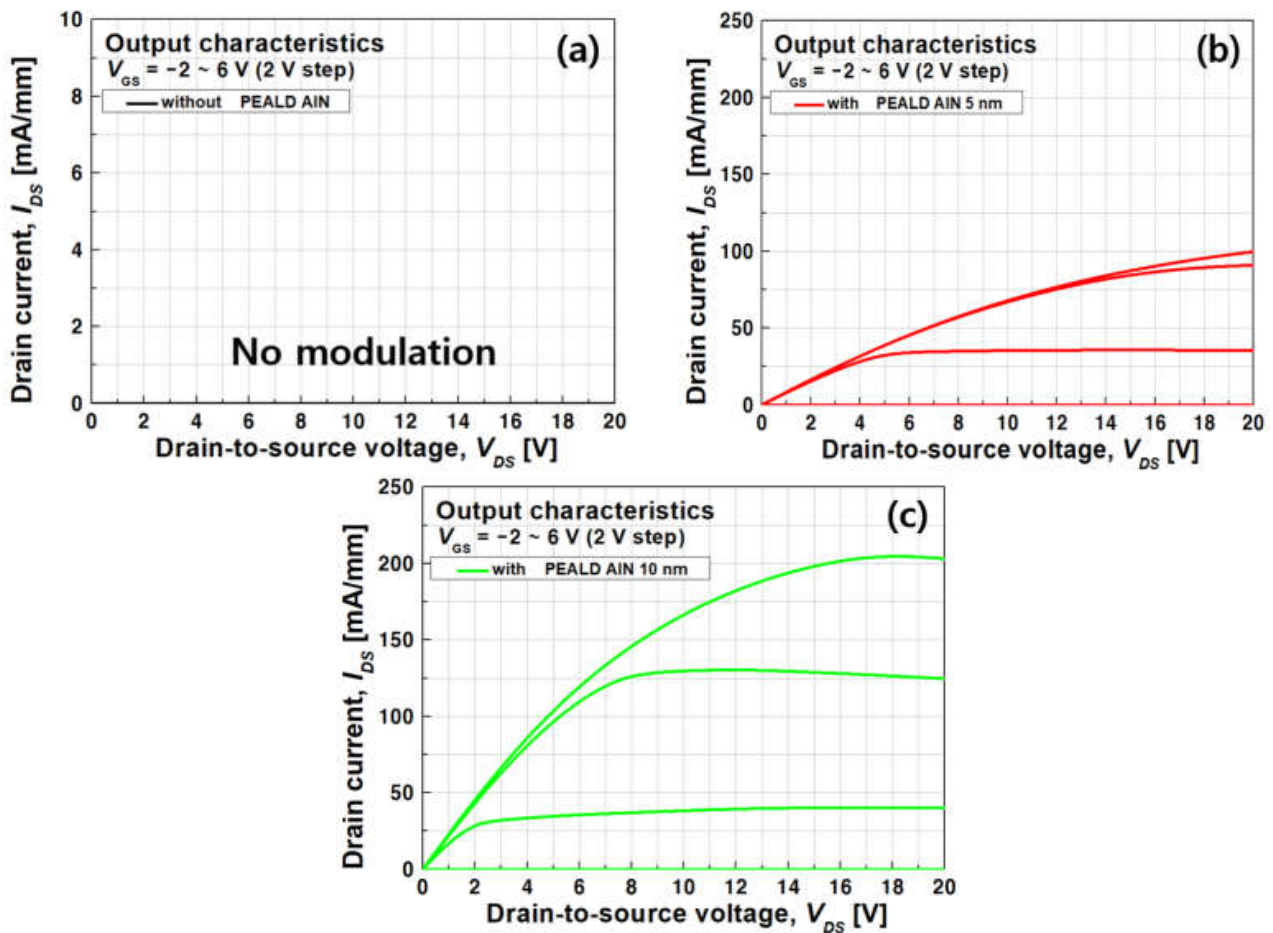


Figure 11. Output current–voltage characteristics of fabricated thin-AlGaIn/GaN MIS-HFETs; (a) without PEALD AlN film, (b) with a 5 nm thick PEALD AlN film, and (c) with a 10 nm thick PEALD AlN film.

The off-state breakdown voltage was evaluated using Keithley 2410 and 2651A source meters with $V_{GS} = 0$ V. As demonstrated in Figure 12, both devices with 5 nm and 10 nm AlN films showed no catastrophic breakdown behavior until 1100 V, which was the maximum limit of our measurement.

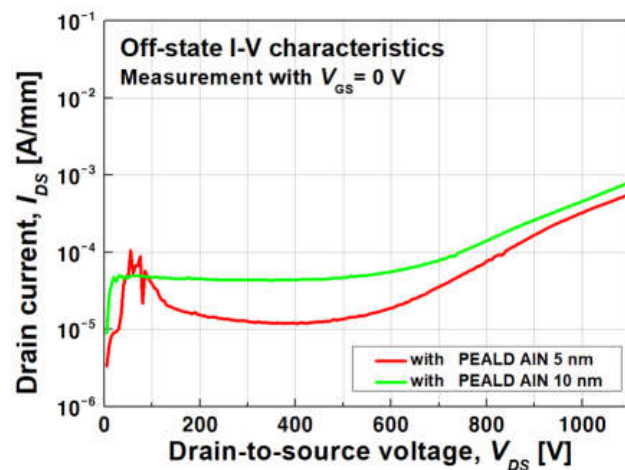


Figure 12. Off-state breakdown characteristics of the fabricated thin-AlGaIn/GaN E-mode MIS-HFET with PEALD AlN films.

3. Conclusions

In this study, the successful fabrication of a thin-AlGa_N/Ga_N MIS-HFET using a crystalline PEALD AlN film was demonstrated. This approach has several advantages, including the elimination of plasma-induced damage and a reduction in gate leakage current. Additionally, the use of a crystalline AlN film was found to enhance the polarization-induced 2DEG channel density, leading to improved electrical properties of the device. Notably, the thickness of the AlN film was found to be a critical factor in determining the device's electrical properties. A thicker film was found to result in increased carrier density and lower sheet resistance. The device fabricated with a 10 nm PEALD AlN film exhibited outstanding E-mode characteristics, including a threshold voltage of 0.45 V, an on/off ratio of approximately 10⁹, a specific on-resistance of 7.1 mΩ·cm², and an off-state breakdown voltage exceeding 1100 V. The results of this study strongly indicate that the crystalline ALD AlN passivation process is essential in achieving excellent device characteristics. The findings of this study offer promising insights into the development of high-performance GaN-based power devices.

Author Contributions: Conceptualization, W.-H.J. and H.-Y.C.; methodology, W.-H.J.; software, W.-H.J.; validation, J.-H.Y., H.K. and H.-Y.C.; formal analysis, W.-H.J.; investigation, W.-H.J.; resources, W.-H.J.; data curation, W.-H.J.; writing—original draft preparation, W.-H.J.; writing—review and editing, H.-Y.C.; visualization, W.-H.J.; supervision, H.-Y.C.; project administration, H.-Y.C.; funding acquisition, H.-Y.C. All authors have read and agreed to the published version of the manuscript.

Funding: This research was funded by National R&D Program (2022M3I8A1085443, 2019M3F5A1A01077147), and Basic Science Research Program (2015R1A6A1A03031833).

Data Availability Statement: Not applicable.

Acknowledgments: This research was supported by National R&D Program (2022M3I8A1085443, 2019M3F5A1A01077147), and Basic Science Research Program (2015R1A6A1A03031833). The authors thank Seunghoon Shin for his support to extract the interface trap density.

Conflicts of Interest: The authors declare no conflict of interest.

References

1. Saito, W.; Takada, Y.; Kuraguchi, M.; Tsuda, K.; Omura, I.; Ogura, T.; Ohashi, H. High breakdown voltage AlGa_N-Ga_N Power-HEMT design and high current density switching behavior. *IEEE Trans. Electron. Devices* **2003**, *50*, 2528–2531. [[CrossRef](#)]
2. Millán, J.; Godignon, P.; Perpiñà, X.; Pérez-Tomás, A.; Rebollo, J. A survey of wide bandgap power semiconductor devices. *IEEE Trans. Power Electron.* **2014**, *29*, 2155–2163. [[CrossRef](#)]
3. Ambacher, O.; Foutz, B.; Smart, J.; Shealy, J.R.; Weimann, N.G.; Chu, K.; Murphy, M.; Sierakowski, A.J.; Schaff, W.J.; Eastman, L.F. Two-dimensional electron gases induced by spontaneous and piezoelectric polarization in undoped and doped AlGa_N/Ga_N heterostructures. *J. Appl. Phys.* **2000**, *87*, 334–344. [[CrossRef](#)]
4. Saadat, O.I.; Chung, J.W.; Piner, E.L.; Palacios, T. Gate-First AlGa_N/Ga_N HEMT technology for high-frequency applications. *IEEE Electron Device Lett.* **2009**, *30*, 1254–1256. [[CrossRef](#)]
5. Oka, T.; Nozawa, T. AlGa_N/Ga_N Recessed MIS-Gate HFET with high-threshold-voltage normally-off operation for power electronics applications. *IEEE Electron Device Lett.* **2008**, *29*, 668–670. [[CrossRef](#)]
6. Jang, W.H.; Seo, K.S.; Cha, H.Y. P-GaN Gated AlGa_N/Ga_N E-mode HFET fabricated with selective GaN etching Process. *J. Semicond. Technol. Sci.* **2020**, *20*, 485–490. [[CrossRef](#)]
7. Huang, S.; Liu, X.; Wang, X.; Kang, X.; Zhang, J.; Bao, Q.; Wei, K.; Zheng, Y.; Zhao, C.; Gao, H. High uniformity normally-off Ga_N MIS-HEMTs fabricated on ultra-thin-barrier AlGa_N/Ga_N Heterostructure. *IEEE Electron. Device Lett.* **2016**, *37*, 1617–1620. [[CrossRef](#)]
8. Huang, S.; Liu, X.; Wang, X.; Kang, X.; Zhang, J.; Fan, J.; Shi, J.; Wei, K.; Zheng, Y.; Gao, H.; et al. Ultrathin-barrier AlGa_N/Ga_N heterostructure: A recess-free technology for manufacturing high-performance Ga_N-on-Si power devices. *IEEE Trans. Electron. Devices* **2018**, *65*, 207–214. [[CrossRef](#)]
9. Kim, H.S.; Kang, M.J.; Jang, W.H.; Seo, K.S.; Kim, H.T.; Cha, H.Y. PECVD Si_N_x passivation for AlGa_N/Ga_N HFETs with ultra-thin AlGa_N barrier. *Solid State Electron.* **2020**, *173*, 107876. [[CrossRef](#)]
10. Zheli, W.; Jianjun, Z.; Yuechan, K.; Cen, K.; Xun, D.; Yang, Y.; Tangsheng, C. Thin-barrier enhancement-mode AlGa_N/Ga_N MIS-HEMT using ALD Al₂O₃ as gate insulator. *J. Semicond.* **2015**, *36*, 094004.
11. Kim, H.-S. Gate Stack and Passivation Engineering for AlGa_N/Ga_N Heterojunction Field-Effect Transistors. Ph.D. Dissertation, Hongik University, Seoul, Republic of Korea, 2020.

12. Hwang, I.H.; Kang, M.J.; Cha, H.Y.; Seo, K.S. Crystalline AlN interfacial layer on GaN using plasma-enhanced atomic layer deposition. *Crystals* **2021**, *11*, 405. [[CrossRef](#)]
13. Deen, D.A.; Champlain, J.G. High frequency capacitance-voltage technique for the extraction of interface trap density of the heterojunction capacitor: Terman's method revised. *Appl. Phys. Lett.* **2011**, *99*, 053501. [[CrossRef](#)]
14. Heikman, S.; Keller, S.; Wu, Y.; Speck, J.S.; Denbaars, S.P.; Mishra, U.K. Polarization effects in AlGaN/GaN and GaN/AlGaN/GaN heterostructures. *J. Appl. Phys.* **2003**, *93*, 10114–10118. [[CrossRef](#)]

Disclaimer/Publisher's Note: The statements, opinions and data contained in all publications are solely those of the individual author(s) and contributor(s) and not of MDPI and/or the editor(s). MDPI and/or the editor(s) disclaim responsibility for any injury to people or property resulting from any ideas, methods, instructions or products referred to in the content.